Assessing the Drought Vulnerability of Alberta: A Deep Learning Approach for Hydro-Climatological Analysis [†]

Vahid Nourani [1,2,*] , Hadi Pourali [1] , Mohammad Bejani [1] and Aida Hosseini Baghanam [1]

[1] Faculty of Civil Engineering, University of Tabriz, Tabriz 51368, Iran; h.pourali1400@ms.tabrizu.ac.ir (H.P.); m.bejani99@ms.tabrizu.ac.ir (M.B.); hosseinibaghanam@tabrizu.ac.ir (A.H.B.)
[2] College of Engineering, Information Technology and Environment, Charles Darwin University, Darwin, NT 0810, Australia
[*] Correspondence: vnourani@yahoo.com
[†] Presented at the 4th International Electronic Conference on Applied Sciences, 27 October–10 November 2023; Available online: https://asec2023.sciforum.net/.

Abstract: This study investigates the vulnerability of Alberta province in Canada to extreme weather events, particularly drought, which has historically caused significant financial losses. Accurate simulating techniques are crucial for obtaining reliable results to identify trends and patterns in Alberta climatology. In this study, 4-monthly synoptic station data spanning 35 years (1979 to 2014) are used alongside Long Short-Term Memory (LSTM) to analyze patterns of precipitation. Additionally, the Standardized Precipitation Index (SPI) is used to identify drought severity at different time scales (3, 6, and 12 months). The results demonstrate that drought occurrences have been observed in the Southern part of Alberta, with rising tendencies in larger areas, such as Calgary agricultural areas, being prone to severe drought.

Keywords: drought; precipitation patterns; Standardized Precipitation Index (SPI); Long Short-Term Memory (LSTM)

1. Introduction

The changing climate is anticipated to lead to more severe drought events and their consequential impacts on both society and the environment [1,2]. Drought occurrences are not limited to specific geographical regions, being widespread across the world and posing challenges in their accurate quantification [3]. Extensive research has investigated the effects of climate change on water discharge patterns and unveiled the possibility of an increased severity of drought events in numerous regions, such as Europe, central North America, Central America, Mexico, northeastern Brazil, and southern Africa [4]. According to [5], there has been a substantial increase in the extent of global regions prone to chronic draughts.

The Standard Precipitation Index (SPI) stands as a widely utilized drought index, considered one of the most popular and accepted ones, originally developed in [6]. The SPI holds several advantages over other drought indices, including consistent spatial interpretation and reduced computational complexity, making it well-suited for prediction and risk analysis [7]. Also, developing an accurate climate model is challenging due to its nonlinear nature [8]. One prominent technique utilized for learning long-term dependencies, especially when dealing with time-series data, is Long-Short-Term-Memory (LSTM), which was introduced in [9] and has demonstrated superior capabilities compared to recurrent neural networks (RNNs) [10].

The main objective of this study is to simulate and determine Alberta's climate pattern using a deep learning LSTM method, and to diagnose the drought vulnerability of Alberta by using the SPI (3, 6, and 12 months) with monthly precipitation data from four gauging stations in the study area, which is depicted in Figure 1. To find out the performances

of the utilized method, the root mean square error (RMSE), as well as the coefficient of determination (DC), are used as performance indicators.
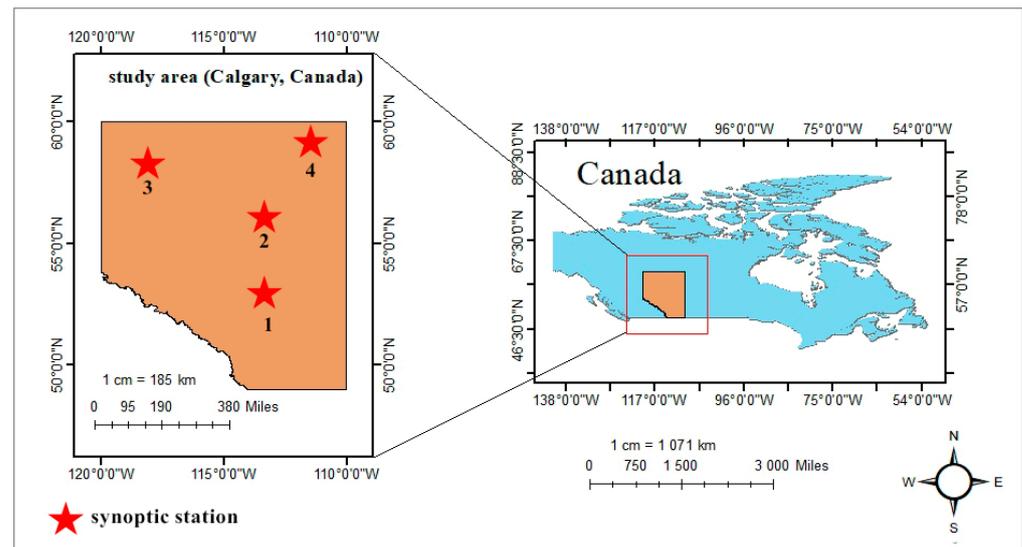
Figure 1. The location of the study area and synoptic stations employed in this study.

2. Methods and Materials

2.1. Study Area and Dataset

Alberta is a Canadian province situated in the southern region, covering an area of 661,000 square kilometers. Figure 1 shows the agricultural areas in the southwestern corner, confined by coordinates 49° N in the south, 110° W in the east, 120° W in the west, and 57° N in the north, spanning approximately 257,848 square kilometers. Agricultural regions in Alberta experience a steppe climate with continental influences. During the hottest days of the year, temperatures can reach up to 30 degrees Celsius or even higher. The region receives an average annual precipitation of approximately 425 mm. Additionally, observational data from four stations located within the regions of the province will be employed, and these data are available on the website www.acis.alberta.ca (accessed on 1 August 2023).

2.2. Standard Precipitation Index (SPI)

The SPI is a prominent drought-monitoring indicator adopted by the World Meteorological Organization [11]. The SPI is a probabilistic measure that relies exclusively on precipitation data and was introduced in [5] to evaluate precipitation deficits in a manner distinctively linked to probability. The SPI is calculated across various accumulation timeframes, typically relying on monthly precipitation data, denoted as SPI-n, where 'n' signifies the number of months over which the accumulation occurs. This calculation can be likened to a moving average, where each month's value is correlated with preceding months, determined by the chosen accumulation timeframe. Negative SPI values indicate drier conditions than what is considered typical for the given timeframe and location, while positive SPI values denote wetter conditions compared to the expected norm for that specific timeframe and location.

The SPI is defined as

$$\text{SPI} = \frac{X_i - \bar{X}}{Sd} \tag{1}$$

where 'X_i' represents the precipitation value for a specific period, 'i'. '$\bar{X}$' denotes the mean precipitation in the historical series for the same period, 'i', while 'Sd' represents the standard deviation of the mean precipitation in that period.

2.3. Long Short-Term Memory

The LSTM network, a specialized type of recurrent neural network (RNN), has been demonstrated to be stable and effective in modeling long-range dependencies [12]. LSTM networks are a type of recurrent neural network with memory blocks containing a cell state, input gate, forget gate, and output gate. The cell state serves as the memory, while the gates control information flow. The input gate manages new input, the forget gate determines what to forget from the previous state, and the output gate decides how to use memory for the output. LSTMs excel at learning from sequential data. For detailed mathematics, refer to [9].

2.4. Evaluation Criteria

In assessing the efficacy of the employed methodologies within this investigation, two evaluation criteria, namely the root mean square error (RMSE) and the coefficient of determination (referred to as DC or Nash–Sutcliffe), were utilized:

$$\text{RMSE} = \sqrt{\frac{\sum_{i=1}^{N} (R_i - Z_i)^2}{N}} \tag{2}$$

$$\text{DC} = 1 - \frac{\sum_{i=1}^{N} (Z_i - R_i)^2}{\sum_{i=1}^{N} \left(Z_i - \bar{Z}\right)^2} \tag{3}$$

where R_i signifies the estimated value, Z_i represents the target value, $\bar{Z}$ stands for the average value of the target observations, and N denotes the size of the sample. The RMSE maintains the same dimension as the observations, whereas the DC is unitless and falls within the range of $(-\infty, 1]$. A higher DC value approaching 1 indicates a greater degree of accuracy in the regression analysis.

3. Results

3.1. Standard Precipitation Index (SPI)

This study aims to monitor drought using the SPI index in Alberta, Canada. In this way, the input data were collected from Alberta's four synoptic stations for the period spanning from 1979 to 2014. Moreover, an LSTM-based statistical downscaling model was used to simulate and assess the suitability of this method for prediction purposes. Since the input data contain missing values, the missing data were filled using the seasonal pattern method; then, the SPI values were calculated at the temporal time scales of 3, 6, and 12 months. The seasonal pattern method first identified the seasonal pattern of observation data, which refers to repeating patterns or trends that occur at regular intervals. Then, the observation data are decomposed into their constituent components. After that, the method inputted missing values in the seasonal component of the data. In the second step, the SPI values were calculated at the time scales of 1, 3, 6, and 12 months in different regions of Alberta.

According to the information provided in Figure 2, it is apparent that the indices for all stations displayed significant fluctuations when observed over shorter periods. However, these fluctuations tended to decrease as the analysis focused on longer time scales. In the context of a 12-month drought period, the first station, as depicted in Figure 2a, experienced its most pronounced drought conditions during the middle and end portions of the statistical period, specifically spanning from 2000 to 2004 and from 2008 to 2010, covering a duration of eight years. Furthermore, according to Figure 2b, at the second station, based on the 12-month drought period, the greatest drought occurred in the middle and end of the reference period (i.e., 1983–1985, 1988–1989, 2000–2003, and 2007–2008) over 11 years. And at the third station (Figure 3c), drought occurred longer than at the first and second stations by 15 years. The drought at this station occurred within the first 5 years, and in the middle and last decade of the statistical period. Finally, in Figure 2d, the longest

drought period happened over 18 years at the fourth station. Similar to the third station, drought events transpired during the initial, middle, and final years of the statistical period. The findings from the SPI analysis reveal that the most severe drought occurrences took place at the first and second stations, three times each, and at the third and fourth stations, two times each. Considering severe drought, all stations experienced the same drought event eight times during the statistical period, and we concluded that the fourth station had the most intense number of drought events and longest periods among others.
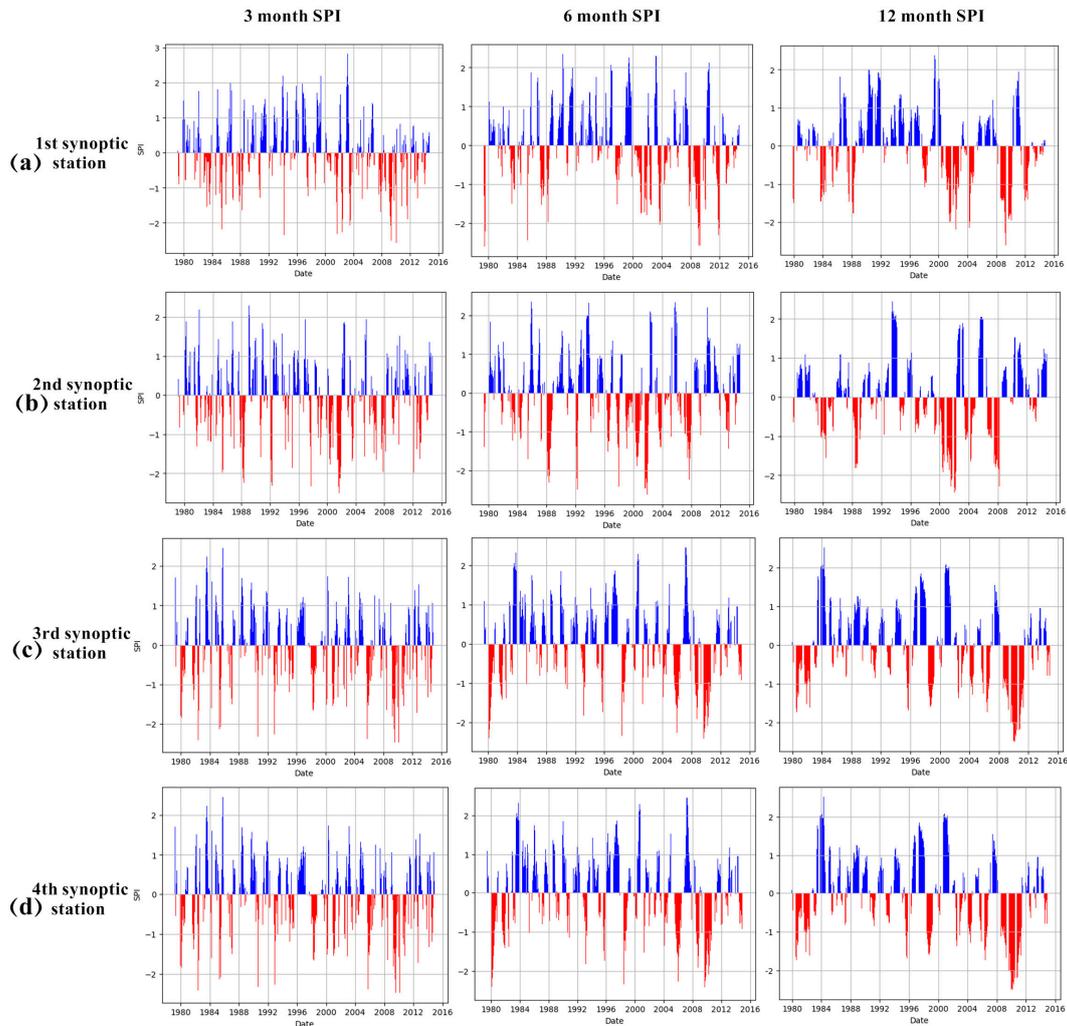
Figure 2. The SPI 3, 6, and 12 indices for 4 synoptic stations of Alberta province, illustrated by (**a**–**d**) in the figure. The blue lines indicate the wetness period and the red lines indicate the dryness period of the region.
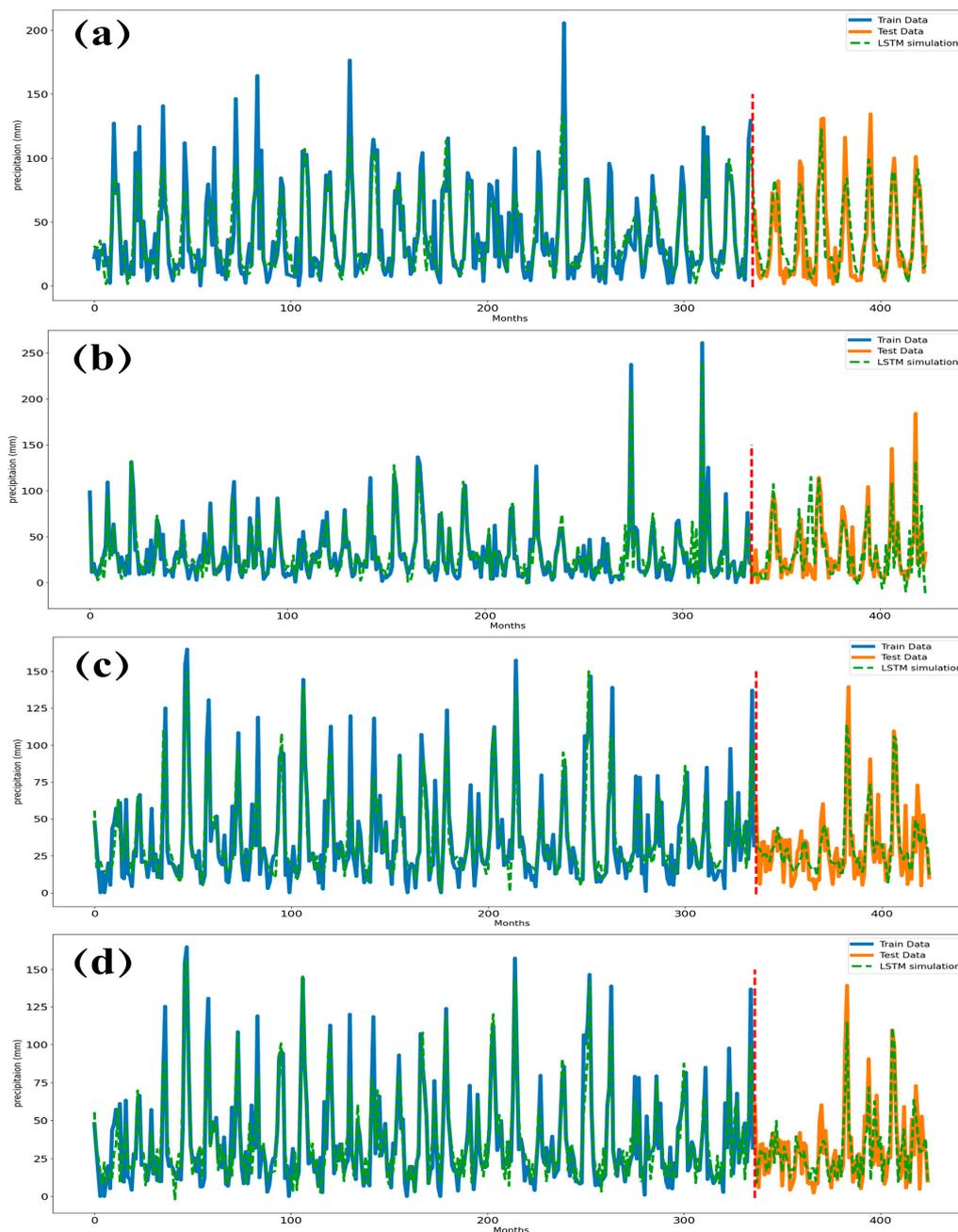
Figure 3. The simulated LSTM precipitation model of Alberta province from 4 synoptic stations, which depicts the stations (**a**–**d**) with an 80-20 split sampling approach for model training and validation, in which the split points are shown as red dots in the figure.

3.2. Statistical Downscaling

The simulation procedure was conducted utilizing an LSTM network, as depicted in Figure 3, with the primary objective of evaluating the suitability of this network for the task at hand.

This epoch utilized a hyperbolic tangent activation function, a batch size of 16, the incorporation of six hidden layers, and assessment using RMSE and DC as evaluation metrics. The dataset was partitioned into two subsets: 80% for training and 20% for testing purposes. The outcomes of the simulation procedure are tabulated in Table 1.

Table 1. The training and validation accuracy of the LSTM model.

Stations	Evaluating Criteria	Training	Validation
Station 1	DC	0.71	0.69
	RMSE (mm)	15.61	18.91
Station 2	DC	0.81	0.78
	RMSE (mm)	13.54	14.95
Station 3	DC	0.79	0.74
	RMSE (mm)	13.90	15.41
Station 4	DC	0.68	0.58
	RMSE (mm)	18.38	19.44

4. Conclusions

Drought, a significant and frequently recurring natural disaster, has detrimental effects on human life. This study aimed to investigate the temporal patterns of drought events spanning from short to long durations in Alberta, Canada. The research utilized the SPI-3, SPI-6, and SPI-12 indices and applied deep-learning LSTM models to simulate Alberta, Canada's, climate. Data from four synoptic weather stations within the study area (1979 to 2014) were used, with an 80-20 split sampling approach for model training and validation. The findings demonstrate the feasibility of employing the LSTM model technique for investigating drought occurrences in Alberta's climate conditions. Additionally, the study noted that as the SPI magnitude increases, there is a noticeable increase in both the intensity and duration of drought incidents, especially within the southern region of Alberta.

References

1. Dai, A. Drought under global warming: A review. *Wiley Interdiscip. Rev. Clim. Chang.* **2011**, *2*, 45–65. [CrossRef]
2. Romm, J. The next dust bowl. *Nature* **2011**, *478*, 450–451. [CrossRef] [PubMed]
3. Wilhite, D.A. *Drought as a Natural Hazard: Concepts and Definitions*; Routledge: London, UK, 2000.
4. Seneviratne, S.I. Historical drought trends revisited. *Nature* **2012**, *491*, 338–339. [CrossRef] [PubMed]
5. Wang, S.Y.; Hipps, L.; Gillies, R.R.; Yoon, J.H. Probable causes of the abnormal ridge accompanying the 2013–2014 California drought: ENSO precursor and anthropogenic warming footprint. *Geophys. Res. Lett.* **2014**, *41*, 3220–3226. [CrossRef]
6. McKee, T.B.; Doesken, N.J.; Kleist, J. The relationship of drought frequency and duration to time scales. In Proceedings of the 8th Conference on Applied Climatology, Anaheim, CA, USA, 17–22 January 1993.
7. Anshuka, A.; van Ogtrop, F.F.; Vervoort, R.W. Drought forecasting through statistical models using standardized precipitation index: A systematic review and meta-regression analysis. *Nat. Hazards* **2019**, *97*, 955–977. [CrossRef]
8. Baghanam, A.H.; Nourani, V.; Bejani, M. AI-Based Statistical Downscaling of Precipitation and Temperature via Convolutional Neural Network Using Nonlinear Predictor Screening Approach. In Proceedings of the International Conference on Natural Resources and Sustainable Environmental Management, Nicosia, Cyprus, 8–12 November 2021; Springer: Cham, Switzerland, 2021.
9. Hochreiter, S.; Schmidhuber, J. Long short-term memory. *Neural Comput.* **1997**, *9*, 1735–1780. [CrossRef] [PubMed]
10. Gers, F. *Long Short-Term Memory in Recurrent Neural Networks*; Ecole Polytechnique Fédérale de Lausanne: Lausanne, Switzerland, 2001. Available online: http://www.felixgers.de/papers/phd.pdf (accessed on 15 September 2023).

11. Svoboda, M.; Hayes, M.; Wood, D. *Standardized Precipitation Index: User Guide*; World Meteorological Organization: Geneva, Switzerland, 2012.
12. Nourani, V.; Sadikoglu, F.; Khodkar, K.; Shahli, A. Downscaling precipitation from GCM parameters using recurrent neural networks. In Proceedings of the International Conference on Theory and Application of Soft Computing, Computing with Words and Perceptions, Antalya, Turkey, 23–24 August 2021.